



## Biosynthesis of Gold Nanoparticles Using Extracts of *Terminalia catappa*, *Hippocratea excelsa*, and Biodegradable Polymers (Pluronic F127 and P103)

Nancy Tepale,<sup>1\*</sup> Eric Flores-Aquino,<sup>2</sup> Víctor Vladimir Amilkar Fernández-Escamilla,<sup>3</sup> Lilia Alejandra Conde-Hernández,<sup>1</sup> Yokiushirdhilmara Estrada-Girón<sup>4</sup>



CrossMark

<sup>1</sup>Facultad de Ingeniería Química, Benemérita Universidad Autónoma de Puebla, Puebla Puebla 72570, México

<sup>2</sup>Departamento de Nanocatálisis, Centro de Nanociencias y Nanotecnología, Universidad Nacional Autónoma de México, Ensenada Baja California 22800, México

<sup>3</sup>Departamento de Ciencias Tecnológicas, Centro Universitario de la Ciénega, Universidad de Guadalajara, Ocotlán Jalisco 47820, México

<sup>4</sup>Departamento de Ingeniería Química, Centro Universitario de Ciencias Exactas e Ingenierías, Universidad de Guadalajara, Guadalajara Jalisco 44430, México

### Abstract

This study aimed to synthesize gold nanoparticles (AuNPs) using *Terminalia catappa* (TC) and *Hippocratea excelsa* (HE) extracts as reducing agents and a triblock copolymer Pluronic (F127 and P103) as the stabilizing agent. The formation of AuNPs was monitored by UV-visible spectroscopy, showing a signature peak between 530 and 540 nm, which corresponds to the Surface Plasmon Resonance (SPR) of AuNPs. As time progressed, the AuNPs synthesized only with the plant extracts showed a decrease in absorbance attributed to particle agglomeration. However, the addition of the copolymer in the reaction changed the behavior of the SPR, and the absorbance level remained almost constant, suggesting stability. This behavior was corroborated by Transmission electron microscopy (TEM). Micrographs showed well-separated spherical nanoparticles when TC extract was used (10-50 nm). However, AuNPs synthesized with HE extract showed spherical templates on whose surface smaller NPs were formed (~10 nm). The hydrodynamic diameter obtained by Dynamic light scattering (DLS) suggests that the biomolecules of the extract and polymer are attached to the nanoparticles. In addition, polyphenols and sesquiterpenes, responsible molecules for reducing Au<sup>3+</sup> and copolymer signals were identified by Fourier transform infrared (FTIR). The results suggest that the copolymer promotes the stability of colloidal solutions and could modify the morphology of AuNPs.

Keywords: Green synthesis; Triblock Copolymer; Extract Plant; Gold Nanoparticles; Stability.

### 1. Introduction

The shape, size, and stability of nanoparticles (NPs) are crucial for their application in several areas, such as cancer treatment, drug transport, agriculture, cosmetics, textiles, contaminated water treatment, and food packaging, among other applications [1], [2], [3], [4]. Therefore, developing new strategies to modify and improve the properties of nanomaterials is a challenge. The most common method for synthesizing metal nanoparticles is the chemical reduction of metal salts in solution. This method usually employs reducing agents such as sodium citrate, citric acid, ascorbic acid, methanol, sodium carbonate, hydrazine, dimethyl formamide, formaldehyde, sodium borohydride, hydrogen, and polymers [5], [6]. These agents are often toxic, hazardous, and non-biodegradable, so in addition to being harmful to the environment, they could also contaminate the surface of the nanoparticles, limiting their applications [3], [6].

There is considerable interest in synthesizing new materials with more efficient and less polluting techniques. Besides, it is also desirable to use water as a solvent in reactions, in addition to less toxic reducing and stabilizing agents [7], [8]. Thus, an alternative to chemical synthesis is green synthesis. Green synthesis or biosynthesis manufactures profitable materials through environmentally friendly processes. Plant biomass can be used in biosynthesis, and to further facilitate this type of synthesis, alternatives such as plant extracts have been proposed [3], [7], [8], [9]. Plant extracts are excellent reducing agents that avoid

\*Corresponding author e-mail: [nancy.tepale@correo.buap.mx](mailto:nancy.tepale@correo.buap.mx); (Nancy Tepale).

Received date 18 June 2024; revised date 02 October 2024; accepted date 15 October 2024

DOI: 10.21608/ejchem.2024.297606.9875

©2025 National Information and Documentation Center (NIDOC)

the problem of toxicity during the reaction [10]. Some biomolecules such as terpenoids, flavonoids, alkaloids, polyphenols, vitamins, amino acids, tannins, polysaccharides, and proteins, are bioreducing agents of great potential [10], [11]. For example, *Terminalia catappa* (TC) leaves are an attractive biological resource in nanoparticle synthesis because they do not have food value. Balaprasad [9] reported the synthesis of AuNPs using only an aqueous extract of TC leaves. The nanoparticles showed a predominantly spherical morphology with an average size of 21 nm. The author suggested that the reduction of metal ions was carried out by the water-soluble acids and tannins present in the extract. In addition, the extract of *Hippocratea excelsa* (HE), a type of root known in Mexico as cancerina, has been used for the same purpose. Nuñez-Delgado *et al.* [7] reported the synthesis of AuNPs using only an aqueous HE extract. The nanoparticles showed a predominantly spherical morphology with a mean size of 25 nm. Different authors have identified sesquiterpenes (hypocratein I, hypocratein II, hypocratein III, and emarginatin A) as the main compounds of HE. However, it also contains other biomolecules such as tingenone, celastrol, pristimerin, excelsin, friedelin, canophylline, canophyllin, canophyllic acid, a-amyrin, b-amyrin, and b-sitosterol. These compounds give the plant anti-inflammatory, antibacterial, antifungal, and anticancer properties [12], [13], [14], [15], [16], [17], [18], [19], [20].

The optimal use of NPs in different applications often depends on their stability. Stabilizing agents such as cetyltrimethylammonium bromide (CTAB) or sodium dodecyl sulphate (SDS) are sometimes required [21], [22]. However, this type of stabilizer can generate cytotoxic residues. Nevertheless, toxicity can be reduced by utilizing biodegradable polymers such as poly lactic acid (PLA), poly(lactic-co-glycolic) acid (PLGA), poly(methyl methacrylate) (PMMA), poly(glycidyl methacrylate) (PGMA), polyaniline (PANI), and poly(ethylene oxide) (PEO) or Pluronic [2], [5], [10], [23], [24].

Reena *et al.* [23] synthesized AuNPs using *Leucas aspera* extract as a reducing agent and the amphiphilic triblock copolymer poly lactic acid-co-polyethylene glycol-co-poly lactic acid (PLA-PEG-PLA) as a stabilizing agent. Utilizing UV-vis spectroscopy, the authors observed a broad absorption band around 540 nm, demonstrating the production of the conjugated nanomaterial. By FTIR spectra, they demonstrated that the nanoparticles and the extract were bound to the polymeric matrix. This conjugation was proved by TEM micrographs. Furthermore, they observed that the extract was perceived as a shadow surrounding the nanoparticles embedded in the polymer. The particles presented a spherical shape and increasing the amount of polymer resulted in smaller particles.

Nanoparticles have a wide range of applications. Therefore, it is desirable to design stable nanomaterials synthesized through environmentally friendly methods. For example, polymers like Pluronic have been used in the NPs simple synthesis [2], [24], [25], [26]. Pluronic is a nonionic block copolymer composed of a central hydrophobic PPO chain with two hydrophilic PEO end chains [27], [28]. These block copolymers function as reducing agents and colloidal stabilizers [26]. Research has shown that PEO and PPO chains are involved in ion reduction and nanoparticle formation. However, PEO plays the leading role, and PPO blocks primarily contribute to stabilization [27]. Additionally, synthesis and stabilization success is highly influenced by the lengths of the hydrophobic and hydrophilic polymer chains. However, to the best of our knowledge, few references employ polymers in the green biosynthesis of AuNPs.

Based on the latter, a simple and environmentally friendly method is proposed here to produce stable AuNPs using the aqueous extract of two plants, *Terminalia catappa* and *Hippocratea excelsa*, as reducing agents. This study proposes to use previously documented plants for the biosynthesis of AuNPs. The reaction conditions established in prior research provide a foundation for introducing modifications, such as incorporating polymers like triblock copolymer F127 and P103, which may enhance the synthesis efficiency regarding physicochemical properties, including size, shape, and stability. The nanoparticles were characterized by UV-visible spectroscopy, TEM, DLS, and FTIR.

## 2. Materials and methods

### 2.1 Materials

Hydrogen tetrachloroaurate (III) hydrate ( $\text{HAuCl}_4 \cdot 3\text{H}_2\text{O}$  99.9%, Sigma Aldrich), triblock copolymers Pluronic F127 ((PEO)<sub>100</sub>-(PPO)<sub>65</sub>-(PEO)<sub>100</sub>) (Sigma Aldrich) and P103 ((PEO)<sub>17</sub>-(PPO)<sub>60</sub>-(PEO)<sub>17</sub>) (BASF), and tri-distilled water (Hycel de México, S.A. de C.V.) were used without further purification. *Terminalia catappa* leaves were collected from a plantation in the Unión de Tecamatlán, municipality of Puebla state, in the east-central area of Mexico. The *Hippocratea excelsa* roots bark was purchased at a local market in Puebla, Mexico.

### 2.2 Preparation of plant extracts

*Terminalia catappa* leaves with similar size, shape, and color were washed with tri-distilled water. They were finely cut and shade-dried at 25 °C for five days. The same procedure was performed for *Hippocratea excelsa*.

For *Terminalia catappa* leaves, 20 g of the powdered plant was placed in 100 mL of tri-distilled water and added into a flask with constant stirring. The mixture was boiled for 10 min. The cooled solution was centrifuged for 5 min at 5,800 rpm to remove solid matter, and then it was filtered through Whatman paper and stored at 4 °C. The extract was used during the first week of

its preparation. For *Hippocratea excelsa* samples, 10 g of small pieces of root bark were placed in a flask with 100 mL of tri-distilled water. The mixture was boiled for 15 min. Once cooled, the solution was centrifuged and filtered following the same procedure as *Terminalia catappa*.

### 2.3 Synthesis of AuNPs

The biosynthesis of AuNPs was performed following methods described by Balaprasad *et al.* [9] and Nuñez-Delgado *et al.* [7], with some modifications. An aqueous extract of *Terminalia Catappa* (1 mL) was used as a reducing agent and was separately added to 20 mL of  $\text{HAuCl}_4 \cdot 3\text{H}_2\text{O}$  aqueous solution (1 mM) in a screw-capped glass flask under stirring at 25 °C for 2 h. The sample was denominated TC AuNPs. Similarly, 1 mL of aqueous extract of *Hippocratea excelsa* was mixed with 10 mL of  $\text{HAuCl}_4 \cdot 3\text{H}_2\text{O}$  (1 mM), and the sample was denominated HE AuNPs. The flasks were covered with aluminum foil to avoid light degradation of samples.

### 2.4 Synthesis of AuNPs using Pluronic

Aqueous solution of F127 at 0.05 wt% was prepared by mixing the copolymer with distilled water under stirring at 25 °C for 12 h. Pluronic F127 was used as a stabilizing agent (1 mL and 10 mL). The copolymeric solution was mixed with the extract of *Terminalia catappa* and added to the gold solution. The samples were labeled as TCF AuNPs. On the other hand, the aqueous solutions of Pluronic P103 (0.05 and 0.5 wt%) were also used as stabilizing agents (1 mL). The samples were prepared by mixing the copolymer with distilled water under stirring at 25 °C for 12 h. The polymeric solution was mixed with the extract of *Hippocratea excelsa* and added to the gold solution. The samples were labeled as HEP AuNPs.

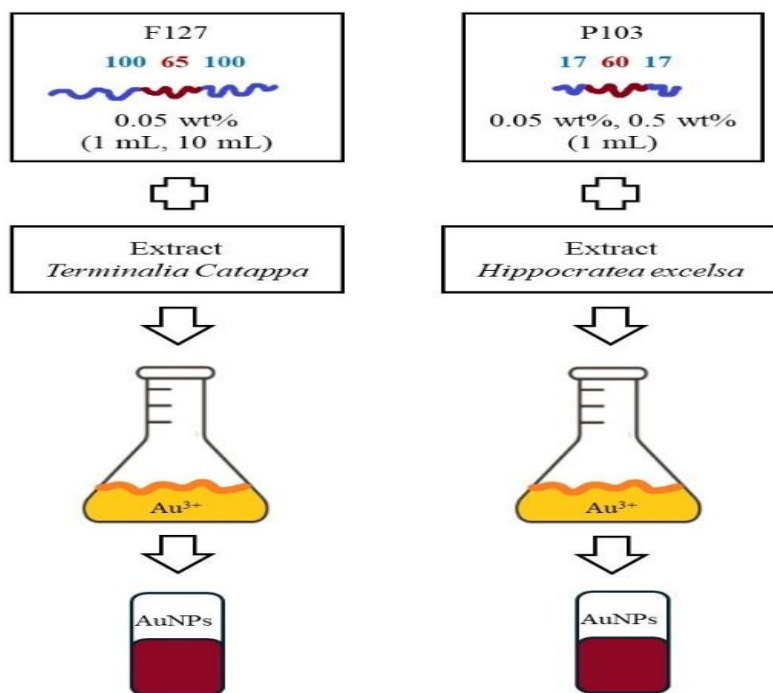


Fig. 1. Flow sheet diagram for preparation of AuNPs using polymers and extract plants.

### 2.5 Characterization

The optical properties of colloidal gold solutions were studied and analyzed by UV-visible spectroscopy using a GENESYS 10S spectrophotometer (Thermo Scientific) at 25°C and quartz cells with an optical path of 1 cm. The size and shape of the AuNPs were determined by TEM analysis using a JEOL-JEM-2010 in conventional transmission mode, operating at 80 kV. For this characterization, samples were prepared by placing a drop of the solution onto a carbon-coated Cu grid.

For HE AuNPs additional techniques were used, the hydrodynamic diameter was measured with a Dynamic Light Scattering System (DLS; Malvern Zetasizer Nano ZS, Malvern Instruments Worcestershire, UK) equipped with a He-Ne laser ( $\lambda = 633$  nm). For these measurements, it was necessary to dilute the sample.

Additionally, a Perkin Elmer Spectrophotometer with a fast Fourier transform and attenuated total reflectance (ATR) system was employed. The scan was carried out in the range of  $4000 - 650 \text{ cm}^{-1}$ . For measurements, the nanoparticles were centrifuged at 6000 rpm for 30 min, washed with acetone, and placed in an ultrasonic bath for 10 min. This procedure was performed twice. Finally, the samples were placed in an oven at  $30 \text{ }^\circ\text{C}$  to evaporate the solvent.

### 3. Results and Discussion

#### 3.1. TC AuNPs

UV-visible spectroscopy is an appropriate technique for monitoring the optical changes that occur during the formation and aggregation of nanoparticles. The absorption spectra of metallic nanoparticles, such as gold, exhibit a strong absorption band corresponding to the SPR. Therefore, this technique is ideal for understanding nanoparticle formation and aggregation. It is also optimal for studying water-soluble nanomaterials [22]. Correlating the plasmonic properties of AuNPs with their morphology is a fast and easy way to monitor the synthesis [29]. Figure 2a depicts the UV-vis absorption spectra of TC AuNPs. The reaction was monitored for 22 days. The spectrum exhibits a remarkable maximal absorbance at 534 nm due to the excitation of surface plasmon vibrations in the gold nanoparticle [9]. The SPR peak absorbance increased to 7 h, suggesting that more nanoparticles were formed [24]. However, after 7 days, the peak decreased, which is associated with aggregation [30]. On day 16, the SPR peak changed shape, and broader peaks indicate the presence of larger-sized particles [29]. Figures 2b and 2c present the representative TEM images obtained on day 16. As seen in the images, the gold nanoparticles are predominantly spherical with sizes from 5 to 35 nm with an average size of  $14 \pm 6.8 \text{ nm}$ . However, the agglomeration of the AuNPs is evident, corroborating what was observed by UV-visible spectroscopy.

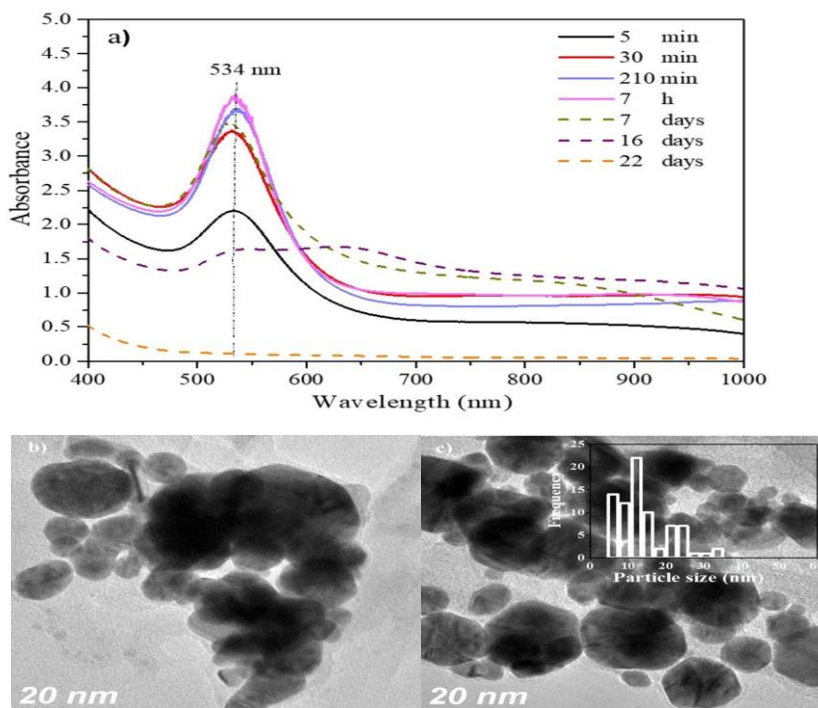


**Fig. 2. (a) The time evolution of the UV-Vis spectra in AuNPs synthesized with *Terminalia catappa* leaf extract (TC AuNPs) at  $25^\circ\text{C}$ ; (b, c) TEM images of TC AuNPs with particle size distribution histogram.**

### 3.2. TC AuNPs using Pluronic F127 (TCF AuNPs)

Figure 3 presents the UV-Vis absorption spectra of TCF AuNPs with and without polymer. The sample TCF1 AuNPs used 1 mL of Pluronic F127, while TCF10 AuNPs used 10 mL. The reaction was monitored for 22 days. Pluronic F127 has been identified as one of the most effective stabilizing agents due to its long hydrophilic PEO block (100 units) [27]. Three colloidal solutions, Figure 3a (7 h of reaction), exhibit absorption bands at approximately 534 nm, indicating the presence of presumably spherical AuNPs [9], [24]. In all three cases, the absorbance remains nearly constant for up to 7 days (Figure 3b). On day 16, the absorbance decreases in all cases (Figure 3c). However, the sample without copolymer (TC AuNPs) diminishes drastically; the band even becomes deformed and widens due to the agglomeration of the nanoparticles, as is observed by TEM in Figures 2b and 2c. When using a higher amount of polymer (TCF10 AuNPs), the absorption band shifts from 534 to 529 nm, suggesting a decrease in particle size. This behavior prevails until day 22. Notably, samples containing polymers maintain their absorbance level, indicating that the polymer confers higher stability (Figure 3d) [30].

In this context, Parry *et al.* [22] synthesized AgNPs using an extract of *Acacia leucophloea* and the addition of CTAB. These authors observed that the SPR was modified, exhibiting a blue shift. The authors related this behavior to the formation of well-dispersed and finer AgNPs. Additionally, Reena *et al.* [23] synthesized AuNPs using the *Leucas aspera* extract as a reducing agent and the PLA-PEG-PLA amphiphilic triblock copolymer as a stabilizing agent. They observed that a higher amount of polymer results in smaller particle sizes. Also, Taha and Da'na [8] reported that *S. argel* leaf extract can reduce  $\text{Au}^{3+}$  ions to  $\text{Au}^0$ . However, by using a biopolymer, the authors had better control over the shape and size of the NPs.

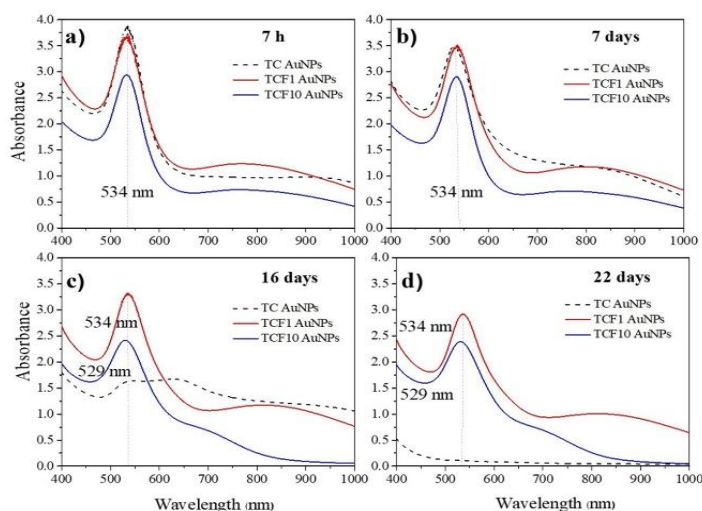


**Fig. 3. Stability of AuNPs using *Terminalia catappa* extract, adding 1 mL (TCF1 AuNPs) and 10 mL (TCF10 AuNPs) of Pluronic F127. (a) 7 h, (b) 7 days, (c) 16 days, and (d) 22 days.**

TEM imaging provided information on the morphology and mean size of AuNPs synthesized with extracts and polymer on day 16. Figure 4a shows NPs synthesized with 1 mL of Pluronic F127 (TCF1 AuNPs). The nanoparticles present quasi-spherical shapes with different sizes (5-50 nm) and an average size of  $25 \pm 13$  nm. Figure 4b presents nanoparticles synthesized with 10 mL of Pluronic F127 (TCF10 AuNPs). These nanoparticles are predominantly spherical, with an average size of  $9.4 \pm 4.6$  nm.

These results corroborate the blue shift demonstrated in the UV-Vis: a higher amount of polymer results in smaller particle sizes. The PEO block has been reported to function mainly as a reducing agent [31]. In the case of F127, the 100 units of PEO plus the biomolecules in the plant extract, could enhance reduction, making the nucleation and nanoparticle formation process more efficient. It is possible that increasing the amount of polymer increases the concentration of reduced  $\text{Au}^{1+}$  ions, generating multiple seeds that promote the formation of small nanoparticles. It is observed that the AuNPs synthesized with 10 mL of

polymeric solution are well distributed (Figure 4b). The polymeric chains may surround the formed particles, separating them efficiently. Therefore, using Pluronic F127 in the synthesis reaction seems to have significant improvement. The AuNPs were smaller and increased their monodispersity and homogeneity. It can be inferred from the TEM images that the presence of polymer has played a critical role in size confinement and has also functioned well as a dispersing and capping agent [32].

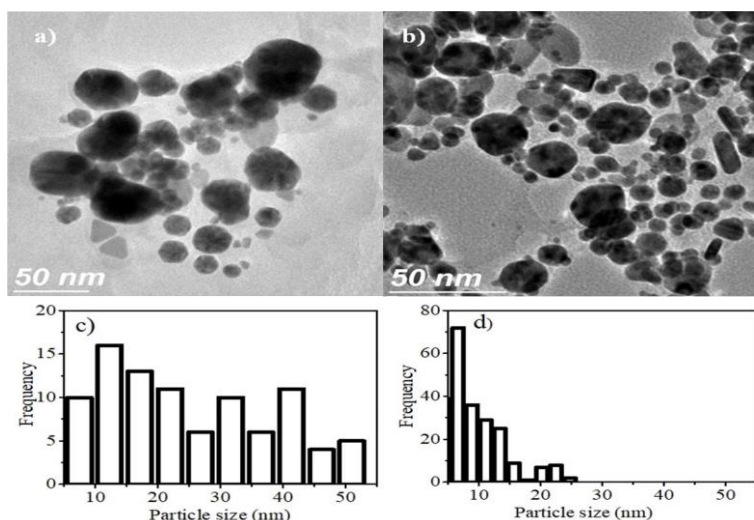


**Fig. 4.** TEM micrographs: (a) AuNPs synthesized with 1 mL (TCF1 AuNPs) of Pluronic F127, and (b) AuNPs synthesized with 10 mL (TCF10 AuNPs) of Pluronic F127. (c, d) Histograms of TCF1 AuNPs and TCF10 AuNPs, respectively.

### 3.3. HE AuNPs

Figure 5a depicts the UV-visible spectrum of AuNPs synthesized with the HE extract. An absorption band is exhibited at about 537 nm, indicating the presence of AuNPs [7], [24]. The absorbance reaches a maximum value within the first hour of the reaction. However, from the seventh day, it decreases considerably. In the micrograph (Figure 5b), the presence of hemispherical NPs with a size of  $37 \pm 16$  nm is observed. Furthermore, the presence of gray shadows attributed to the extract is remarkable.

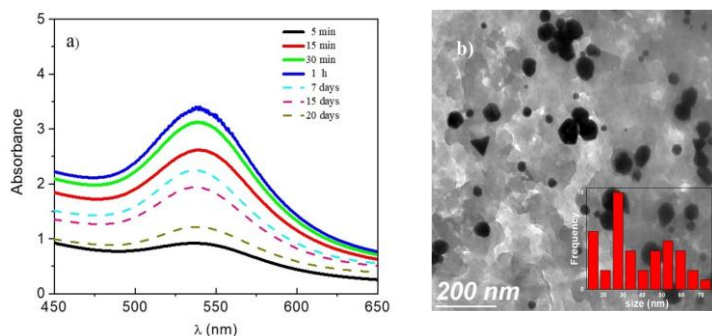


**Fig. 5.** (a) The time evolution of the UV-Vis spectra of HE AuNPs at 25°C; (b) TEM image on day 16 with particle size distribution histogram.

### 3.4. HE AuNPs using Pluronic P103 (HEP AuNPs)

The synthesis of AuNPs employing HE extract was studied with Pluronic P103. At a certain concentration, this copolymer forms micelles (critical micelle concentration, *cmc*), and it has been used to synthesize AuNPs and AgNPs following green chemistry principles [2].

Figure 6 presents the absorbance vs. time of HEP AuNPs with Pluronic P103 at 0.05 wt% (concentration below the *cmc*) and 0.5 wt% (concentration above *cmc*). The copolymer incorporation maintains the absorbance levels, especially after the seventh day (10,000 min).

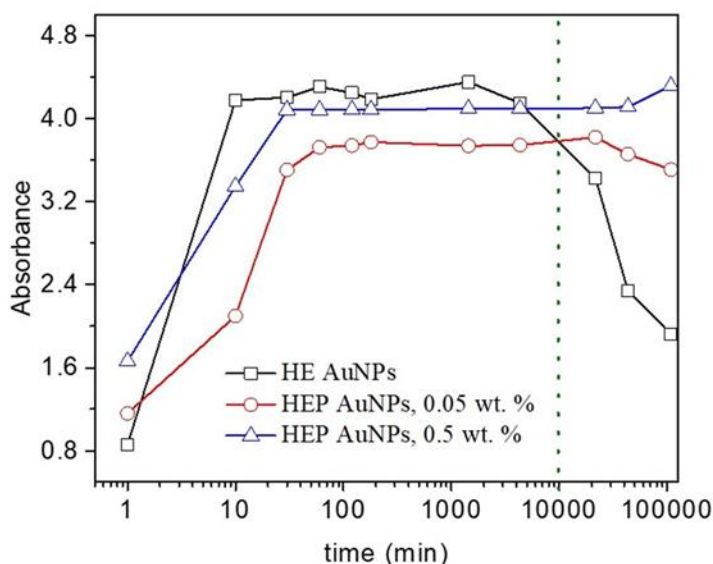
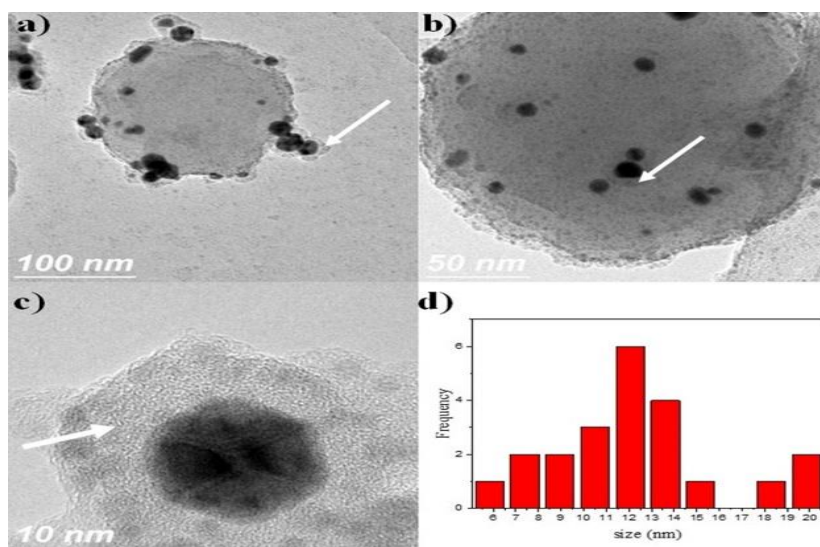
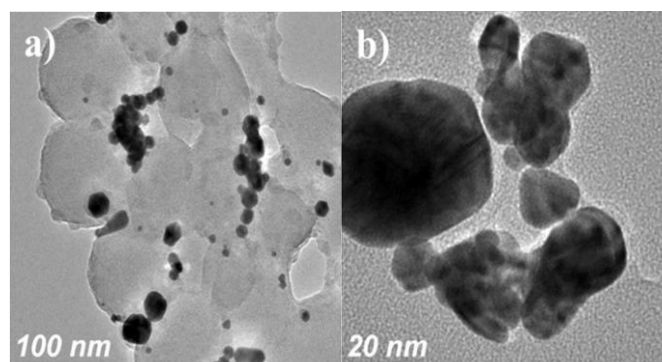


Fig. 6. Kinetic of AuNPs formation at 25 °C, the solid lines are visual aids.

Figure 7 shows TEM images of the HEP AuNPs sample prepared at 0.05 wt% of Pluronic P103 and 25 °C. The copolymer promotes the formation of spherical templates on whose surface smaller NPs are formed (Figures 7a and 7b). Therefore, the morphology of AuNPs has changed, and they were entrapped by the hydrophobic side of the amphiphilic block copolymer [1]. Additionally, it is possible to observe that AuNPs possess a protective layer (indicated with an arrow), suggesting synergy between the extract and P103 triblock copolymer [5]. The average size of the NPs is  $12.2 \text{ nm} \pm 3.7 \text{ nm}$ . Figure 8 presents TEM images of HEP AuNPs prepared at 0.5 wt% of Pluronic P103 and 25 °C. An increase in polymer concentration promotes the agglomeration of the templates and nanoparticles, resulting in irregular shapes with different sizes. These results show that the concentration of the polymer drives the synthesis of nanomaterials [23]. It is essential to highlight that when plant extract is solely used as a reducing agent, the NPs obtained are independent and dispersed in the medium, with sizes ranging from 5 to 70 nm, depending on the extract used. However, when polymers are used, their structures are modified. In the case of Pluronic F127, the nanoparticles observed in Figure 4 suggest that the long blocks of 100 PEO units, in synergy with the plant extract molecules, promote the nucleation process, generating isolated and stabilized NPs. On the other hand, Pluronic P103 has only 17 units in the PEO block and has been reported to be able to form soft templates in the synthesis of metallic nanoparticles [2]. Other copolymers with similar PEO structures, such as P123, have also been observed to form templates [33]. Therefore, the presence of this polymer generates multiple nucleation centers or small pseudo-crown ether cavities where the reduction of gold ions takes place. Once  $\text{Au}^0$  is produced, several  $\text{Au}^0$  are available in nanosized cavities [31].



**Fig. 7.** (a-c) TEM images of HEP AuNPs prepared at 0.05 wt% and 25 °C, (d) particle size distribution histogram.



**Fig. 8.** Micrographs at 100 and 20 nm using the P103 copolymer at 0.5 wt% and 25 °C.

The hydrodynamic diameter was monitored for 15 days through the DLS technique. The hydrodynamic diameter measures the diameter of the NPs, including any stabilizing molecules attached to their surface [34]. Figure 9 shows the size of the NPs synthesized with and without copolymer. On the first day, the NPs without copolymer have an approximate size of 120 nm, and with time, their size increases. On the other hand, NPs synthesized with copolymer exhibit a larger size from the beginning. When the copolymer is added at a concentration below the *cmc* (presence of monomers), the size of the polymer-NPs conjugate is almost constant. Increasing the copolymer concentration reveals that the polymer structure affects the overall size of the nanostructures.

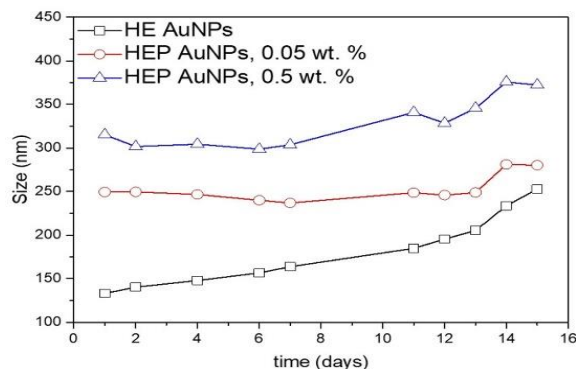


Fig. 9. Size distribution of HE-AuNPs and HEP-AuNPs.

Figure 10 displays the FTIR spectra of the HE extract, HE AuNPs, and HEP AuNPs (P103 at 0.05 wt%). The high concentration of polyphenols in the extract (HE) is confirmed by the OH stretching vibrations assigned to the vibrations of hydroxyl groups in phenols ( $3100 - 3400 \text{ cm}^{-1}$ ) and by the presence of the stretching vibration of aliphatic C-H bonds ( $2848-2934 \text{ cm}^{-1}$ ) and -OH bending vibrations ( $1600-1630 \text{ cm}^{-1}$ ) [34], [35], [36], [37]. The intensive absorption band at  $1040 \text{ cm}^{-1}$  is attributed to the stretching vibrations of C-O-C bonds. Even this signal in previous studies has been attributed to a sesquiterpene [14], [15]. The spectrum of HE AuNPs shows a slight variation, which indicates the presence of residual extract as a reduction agent in the reaction [36], [38]. It can be inferred that alcohols are the main constituents of the HE extract and are mainly responsible for the reduction and stabilization of NPs [37]. On the other hand, the spectrum of HEP AuNPs shows the existence of methyl groups in Pluronic P103 ( $2970$  and  $1373 \text{ cm}^{-1}$ ). The band at  $2970 \text{ cm}^{-1}$  is assigned to the antisymmetric C-H stretching vibration of methyl groups in the PPO blocks, and that identified at  $1373 \text{ cm}^{-1}$  is assigned to the symmetric deformation band of methyl groups [39], [40]. We demonstrated by FTIR spectra analysis that the nanoparticles and the extract are bound to the polymeric matrix. As previously discussed, the conjugation of the nanoparticles with the polymeric matrix was demonstrated with TEM micrographs.

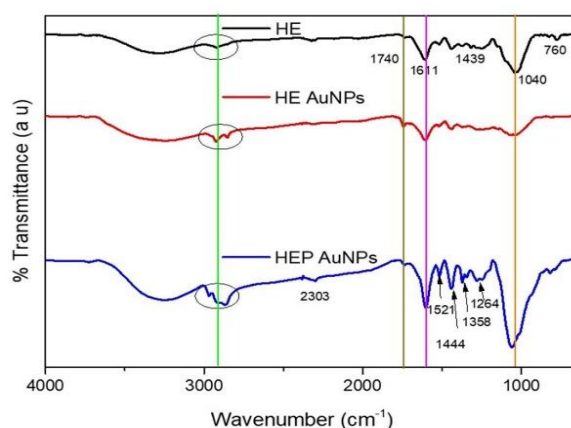


Fig. 10. FTIR spectra of HE extract and AuNPs with and without polymer.

#### 4. Conclusion

The UV-Vis spectral analysis showed NPs formation when we used *Terminalia catappa* and *Hippocratea excelsa* extracts as reducing agents. However, it has been revealed that AuNPs agglomerate over time, losing their colloidal stability. Therefore, biodegradable polymers like Pluronic F127 or P103 have been used to modify the structure and stability of the NPs in the reaction medium. Nonetheless, the response of the system depends on the extract used. The nature of biomolecules in plant extracts is a critical factor in biosynthesis.

Better performance of the *Terminalia catappa* and *Hippocratea excelsa* extract was observed when the polymer was added. In the first case, the NPs produced are mostly spherical with smaller sizes, as confirmed by TEM. *Terminalia catappa* extract acted as a reducing agent and partial stabilizer in the NPs synthesis. Stabilization efficiency increased enormously with the incorporation of Pluronic F127. In the second case, organic matter and the Pluronic P103 promoted the formation of soft templates on whose surface tiny NPs were generated.

The results suggest that the copolymer promotes the stability of colloidal solutions and could modify the morphology of AuNPs. This combinatorial approach allows the design of stable AuNPs; their stability and ease of preparation, combined with their size and spherical shape, make them a promising eco-friendly synthesis method that opens new research possibilities. The exploration of nanostructures integrating poly(ethylene oxide)-poly(propylene)-poly(ethylene oxide) (PEO-PPO-PEO) and metal nanoparticles is gaining prominence as a significant research domain due to their varied applications in areas such as catalysis and medicine.

#### 5. Conflicts of interest

The authors declare that there is no conflict of interest regarding the publication of this manuscript.

#### 6. Funding source

This work was supported by the VIEP-BUAP 2023-2024 as supported by the VIEP-BUAP 2023-2024.

#### 7. Acknowledgments

The authors are very grateful to Francisco Ruiz and Jaime Mendoza for their technical support with TEM measurements at CNyN-UNAM.

#### 8. References

- [1] O. S. Muddineti, B. Ghosh, and S. Biswas, "Current trends in using polymer coated gold nanoparticles for cancer therapy," *International Journal of Pharmaceutics*, vol. 484, no. 1–2, pp. 252–267, Apr. 2015. doi: 10.1016/j.ijpharm.2015.02.038.
- [2] F. K. Rivas-Moreno et al., "Effect of pluronic P103 concentration on the simple synthesis of Ag and Au nanoparticles and their application in anatase-TiO<sub>2</sub> decoration for its use in photocatalysis," *Molecules*, vol. 27, no. 127, Jan. 2022, doi: 10.3390/molecules27010127.
- [3] S. S. Salem and A. Fouda, "Green Synthesis of Metallic Nanoparticles and Their Prospective Biotechnological Applications: an Overview," *Biol Trace Elem Res*, vol. 199, pp. 344–370, 2021, doi: 10.1007/s12011-020-02138-3.
- [4] A. Andleeb et al., "A systematic review of biosynthesized metallic nanoparticles as a promising anti-cancer-strategy," *Cancers*, vol. 13, no. 2818, Jun, 2021, doi: 10.3390/cancers13112818.
- [5] K. Chitra, K. Reena, A. Manikandan, and S. A. Antony, "Antibacterial studies and effect of poloxamer on gold nanoparticles by zingiber officinale extracted green synthesis," *J Nanosci Nanotechnol*, vol. 15, no. 7, pp. 4984–4991, Jul. 2015, doi: 10.1166/jnn.2015.10023.
- [6] M. N. Alam, N. Roy, D. Mandal, and N. A. Begum, "Green chemistry for nanochemistry: Exploring medicinal plants for the biogenic synthesis of metal NPs with fine-tuned properties," *RSC Advances*, vol. 3, no. 30, pp. 11935–11956, Aug. 2013, doi: 10.1039/c3ra23133j.
- [7] C. Nuñez-Delgado, A. Luna-Flores, L. A. Conde-Hernández, E. Flores-Aquino, A. Romero-López, and N. Tepale, "Biosynthesis of gold nanoparticles using the aqueous extract of *Hippocratea excelsa* root bark. Antioxidant and photocatalytic evaluation," *Revista Mexicana de Ingeniería Química*, vol. 22, no. 3, 2023, doi: 10.24275/rmiq/IA2367.
- [8] A. Taha and E. Da'na, "Phyto-Assisted Assembly of Metal Nanoparticles in Chitosan Matrix Using *S. argel* Leaf Extract and Its Application for Catalytic Oxidation of Benzyl Alcohol," *Polymers (Basel)*, vol. 14, no. 776, Feb. 2022, doi: 10.3390/polym14040766.
- [9] B. Ankamwar, "Biosynthesis of Gold Nanoparticles (Green-gold) Using Leaf Extract of *Terminalia Catappa*," *E-Journal of Chemistry*, vol. 7, p. 745120, 2010, doi: 10.1155/2010/745120.
- [10] P. Kumari, S. Luqman, and A. Meena, "Application of the combinatorial approaches of medicinal and aromatic plants with nanotechnology and its impacts on healthcare," *DARU, Journal of Pharmaceutical Sciences*, vol. 27, no. 1, pp. 475–489, Jun. 2019, doi: 10.1007/s40199-019-00271-6.

- [11] M. Ovais et al., "Role of plant phytochemicals and microbial enzymes in biosynthesis of metallic nanoparticles," *Applied Microbiology and Biotechnology*, vol. 102, pp. 6799–6814, Aug. 2018, doi: 10.1007/s00253-018-9146-7.
- [12] R. Reyes-Chilpa et al., "Natural Insecticides from *Hippocratea excelsa* and *Hippocratea celastroides*," *Econ Bot*, vol. 57, no. 1, pp. 54–64, 2003, [Online]. Available: <http://www.jstor.org/stable/4256642>
- [13] D. Cáceres-Castillo, G. J. Mena-Rejón, R. Cedillo-Rivera, and L. Quijano, "21 $\beta$ -Hydroxy-oleanane-type triterpenes from *Hippocratea excelsa*," *Phytochemistry*, vol. 69, no. 4, pp. 1057–1064, Feb. 2008, doi: 10.1016/j.phytochem.2007.10.016.
- [14] F. Calzada and R. Mata, "Hippocrateine III, A Sesquiterpene Alkaloid From *Hippocratea Excelsa*," *Phytochemistry*, vol. 40, no. 2, pp. 583–585, 1995, doi.org/10.1016/0031-9422(95)00255-6.
- [15] R. Mata, F. Calzada, E. Díaz, and R. A. Toscano, "Chemical Studies on Mexican Plants Used in Traditional Medicine, XV. Sesquiterpene Evonoinate Alkaloids from *Hippocratea excelsa*," *J. Nat. Prod.*, vol. 53, no. 5, pp. 1212–1219, 1990.
- [16] M. Furukawa, M. Furukawa, M. Makino, T. Uchiyama, Y. Fujimoto, and K. Matsuzaki, "New sesquiterpene pyridine alkaloids from *hippocratea excelsa*," *Nat Prod Commun*, vol. 13, no. 8, pp. 957–960, Aug. 2018, doi: 10.1177/1934578x1801300809.
- [17] M. Furukawa, M. Makino, T. Uchiyama, K. Ishimi, Y. Ichinohe, and Y. Fujimoto, "Sesquiterpene pyridine alkaloids from *Hippocratea excelsa*," *Phytochemistry*, vol. 59, no. 7, pp. 767–777, 2002, doi: 10.1016/S0031-9422(02)00020-1.
- [18] G. J. Mena-Rejón et al., "Antigiardial activity of triterpenoids from root bark of *Hippocratea excelsa*," *J Nat Prod*, vol. 70, no. 5, pp. 863–865, May 2007, doi: 10.1021/np060559y.
- [19] A. Navarrete, J. Trejo-Miranda, and L. Reyes-Trejo, "Principles of root bark of *Hippocratea excelsa* (Hippocrataceae) with gastroprotective activity," *J Ethnopharmacol.*, vol. 79, no. 3, pp. 383–388, 2002, doi: 10.1016/s0378-8741(01)00414-7.
- [20] R. Perez, S. Perez, M. Zavala, and M. Salazar, "Anti-inflammatory activity of the bark of *Hippocratea excelsa*," *J Ethnopharmacol.*, vol. 47, no. 2, pp. 85–90, 1995, doi: 10.1016/0378-8741(95)01257-e.
- [21] Z. Khan, O. Bashir, J. I. Hussain, S. Kumar, and R. Ahmad, "Effects of ionic surfactants on the morphology of silver nanoparticles using Paan (Piper betel) leaf petiole extract," *Colloids Surf B Biointerfaces*, vol. 98, pp. 85–90, Oct. 2012, doi: 10.1016/j.colsurfb.2012.04.033.
- [22] S. H. Parrey et al., "Green synthesis of silver nanoparticles using *Acacia leucophloea* in the presence of cetyltrimethylammonium bromide and their antibacterial activity," *Colloid Polym Sci*, vol. 300, pp. 835–849, Jul. 2022, doi: 10.1007/s00396-022-04995-x.
- [23] K. Reena, P. Balashanmugam, M. Gajendiran, and S. Arul Antony, "Synthesis of leucas aspera extract loaded gold-PLA-PEG-PLA amphiphilic copolymer nanoconjugates: In vitro cytotoxicity and anti-inflammatory activity studies," *J Nanosci Nanotechnol*, vol. 16, no. 5, pp. 4762–4770, May 2016, doi: 10.1166/jnn.2016.12404.
- [24] M. Sokolsky-Papkov and A. Kabanov, "Synthesis of well-defined gold nanoparticles using Pluronic: The role of radicals and surfactants in nanoparticles formation," *Polymers (Basel)*, vol. 11, no. 1553, Oct. 2019, doi: 10.3390/polym11101553.
- [25] T. Sakai and P. Alexandridis, "Mechanism of gold metal ion reduction, nanoparticle growth and size control in aqueous amphiphilic block copolymer solutions at ambient conditions," *Journal of Physical Chemistry B*, vol. 109, no. 16, pp. 7766–7777, Apr. 2005, doi: 10.1021/jp046221z.
- [26] T. Sakai, Y. Horiuchi, P. Alexandridis, T. Okada, and S. Mishima, "Block copolymer-mediated synthesis of gold nanoparticles in aqueous solutions: Segment effect on gold ion reduction, stabilization, and particle morphology," *J Colloid Interface Sci*, vol. 394, no. 1, pp. 124–131, Mar. 2013, doi: 10.1016/j.jcis.2012.12.003.
- [27] T. Simon, S. C. Boca, and S. Astilean, "Pluronic-Nanogold hybrids: Synthesis and tagging with photosensitizing molecules," *Colloids Surf B Biointerfaces*, vol. 97, pp. 77–83, Sep. 2012, doi: 10.1016/j.colsurfb.2012.03.037.
- [28] D. C. Santos, V. C. de Souza, D. A. Vasconcelos, G. R. S. Andrade, I. F. Gimenez, and Z. Teixeira, "Triblock copolymer-mediated synthesis of catalytically active gold nanostructures," *Journal of Nanoparticle Research*, vol. 20, no. 4, Apr. 2018, doi: 10.1007/s11051-018-4212-8.
- [29] S. M. Rakib-Uz-Zaman et al., "Biosynthesis of Silver Nanoparticles from *Cymbopogon citratus* Leaf Extract and Evaluation of Their Antimicrobial Properties," *Challenges*, vol. 13, no. 1, p. 18, May 2022, doi: 10.3390/challe13010018.
- [30] M. Ahani and M. Khatibzadeh, "Green synthesis of silver nanoparticles using gallic acid as reducing and capping agent: effect of pH and gallic acid concentration on average particle size and stability," *Inorganic and Nano-Metal Chemistry*, vol. 52, no. 2, pp. 234–240, 2022, doi: 10.1080/24701556.2021.1891428.
- [31] M. S. Bakshi, A. Kaura, P. Bhandari, G. Kaur, K. Torigoe, and K. Esumi, "Synthesis of colloidal gold nanoparticles of different morphologies in the presence of triblock polymer micelles," *Journal of Nanoscience and Nanotechnology*, vol. 6, pp. 1405–1410, May 2006, doi: 10.1166/jnn.2006.196.
- [32] L. S. B. Upadhyay and N. Kumar, "Green synthesis of copper nanoparticle using glucose and polyvinylpyrrolidone (PVP)," *Inorganic and Nano-Metal Chemistry*, vol. 47, no. 10, pp. 1436–1440, Oct. 2017, doi: 10.1080/24701556.2017.1357576.
- [33] P. Chatterjee and S. Hazra, "pH-dependent size and structural transition in P123 micelle induced gold nanoparticles," *RSC Adv*, vol. 5, no. 85, pp. 69765–69775, Jul. 2015, doi: 10.1039/c5ra12090j.
- [34] R. Rey-Méndez, M. C. Rodríguez-Argüelles, and N. González-Ballesteros, "Flower, stem, and leaf extracts from *Hypericum perforatum* L. to synthesize gold nanoparticles: Effectiveness and antioxidant activity," *Surfaces and Interfaces*, vol. 32, no. 102181, Aug. 2022, doi: 10.1016/j.surfin.2022.102181.
- [35] M. Irfan, T. Ahmad, M. M. Moniruzzaman, B. B. Abdullah, and S. Bhattacharjee, "Ionic Liquid Mediated Biosynthesis of Gold Nanoparticles Using *Elaeis Guineensis* (Oil Palm) Leaves Extract," *Procedia Eng*, vol. 148, pp. 568–572, 2016, doi: <https://doi.org/10.1016/j.proeng.2016.06.512>.
- [36] R. Mariychuk, D. Grulova, L. M. Grishchenko, R. P. Linnik, and V. V. Lisnyak, "Green synthesis of non-spherical gold nanoparticles using *Solidago canadensis* L. extract," *Applied Nanoscience (Switzerland)*, vol. 10, no. 12, pp. 4817–4826, Dec. 2020, doi: 10.1007/s13204-020-01406-x.
- [37] M. F. Zayed, R. A. Mahfoze, S. M. El-kousy, and E. A. Al-Ashkar, "In-vitro antioxidant and antimicrobial activities of metal nanoparticles biosynthesized using optimized *Pimpinella anisum* extract," *Colloids Surf A Physicochem Eng Asp*, vol. 585, no. 124167, Jan. 2020, doi: 10.1016/j.colsurfa.2019.124167.

- 
- [38]R. Karamian and J. Kamalnejad, "Green Synthesis of Silver Nanoparticles Using Cuminum cyminum Leaf Extract and Evaluation of Their Biological Activities," *J Nanostruct*, vol. 9, no. 1, pp. 74–85, 2019, doi: 10.22052/JNS.2019.01.008.
- [39]A. Sarhan, "Synthesis, spectroscopic investigation and bactericidal effect of poly (Vinyl Alcohol) (PVA) - Iron nanoparticles (Fe Nps)," *Egypt J Chem*, vol. 63, no. 11, pp. 4659–4670, Nov. 2020, doi: 10.21608/EJCHEM.2020.34685.2725.
- [40]Y.-L. Su, J. Wang, and H.-Z. Liu, "Formation of a Hydrophobic Microenvironment in Aqueous PEO-PPO-PEO Block Copolymer Solutions Investigated by Fourier Transform Infrared Spectroscopy," *J. Phys. Chem. B*, vol. 106, no. 45, pp. 11823–11828, 2002, doi: 10.1021/jp026160.